Transposon-sequencing across multiple *Mycobacterium abscessus* isolates reveals significant functional genomic diversity among strains

Chidiebere Akusobi[1] Bouchra S. Benghomari[2], Sanjeevani Choudhery[3], Shreya Singhvi[4], Allison Hicks[1], Thomas R. Ioerger[3], Eric J. Rubin[1]

[1]Department of Immunology and Infectious Diseases, Harvard T.H. Chan School of Public Health, Boston, MA 02115, USA

[2]Department of Biology, Northeastern University, Boston, MA 02115 USA

[3]Department of Computer Science and Engineering, Texas A&M University, College Station Texas 77843,

[4]Department of Molecular and Cell Biology, University of California, Berkeley, Berkeley, CA 94720 USA

USA

Abstract

Mycobacterium abscessus (Mab) clinical isolates have large accessory genomes that are comprised of plasmids, prophages, and genomic islands acquired by horizontal gene transfer. Due to their large accessory genomes*, Mab* clinical isolates are highly genetically diverse. The functional consequence of this diversity remains largely unknown because to date, functional genomic studies in *Mab* have largely been performed on reference strains. Given the growing public health threat of *Mab* infections, understanding the functional genomic differences among *Mab* clinical isolates can provide more insight into how its genetic diversity influences gene essentiality and clinically relevantly phenotypes. To determine the functional genomic diversity among *Mab* strains, we conducted transposon-sequencing (TnSeq) on 22 genetically diverse clinical isolates. We generated triplicate libraries for 16 *M. abscessus subspecies abscessus* isolates and single libraries for 6 *M. abscessus subspecies massiliense* isolates, cataloguing all the essential and non-essential genes in each strain. We identified 562 genes that were differentially required across the 22 clinical isolates, representing ~15% of the *Mab* core genome. We also identified genes whose requirements were sub-species, lineage, and isolate specific. Finally, we identified 10,198 pairs of genes whose genetic requirements were significantly correlated and ultimately identified 19 previously uncharacterized genetic networks in *Mab*. Altogether, this study is the first to unveil differences in genetic requirement across *Mab* clinical isolates and establishes that *Mab* strains are not only genetically diverse, but also functionally diverse as well.

Introduction

Mycobacterium abscessus (Mab) has emerged in recent years as a growing threat to public health due to the rise of *Mab* infections worldwide (1). *Mab* causes a wide range of infections including 80% of pulmonary infections from rapidly growing mycobacteria (2,3). Treating *Mab* infections is difficult due to *Mab's* high level of intrinsic resistance to many antibiotics, including most of the cornerstones of tuberculosis treatment (4–7). Importantly, treating *Mab* requires identifying the sub-species of the clinical isolate, which influences antibiotic treatment based on the presence of *erm*, a gene that confers inducible macrolide resistance (8,9).

Mab is divided into three sub-species: *abscessus, bolletii,* and *massiliense* (10,11). Notably, the majority of *massiliense* sub-species lack an active *erm* gene (8,9). Whole-genome sequencing of *Mab* clinical isolates revealed that *Mab* has a large, open pan-genome, with isolates sharing ~70% of their genome in what is known as the 'core genome' (12,13). The remaining 30% of gene content is in the 'accessory genome' defined as genes present in some clinical isolates, but not all. The majority of accessory genome content is comprised of plasmids, prophages, and genomic islands acquired by horizontal gene transfer (HGT) (14). Unlike *Mycobacterium tuberculosis (Mtb),* which evolves clonally likely due to its facultative intracellular lifestyle (15), the primary driver of *Mab* evolution is recombination and HGT (12,16,17). As a result, compared to TB, *Mab* clinical isolates have larger accessory genomes, which are significant contributors to the genetic diversity present in this species.

While *Mab* clinical isolates have large accessory genomes, the functional consequence of this diversity remains unknown. Previous studies have shown that accessory gene content impacts genetic networks generating new phenotypes, gene dependencies, and redundancies within strains (18–20). Variation in accessory genomes likely generates functional genomic and phenotypic differences between isolates. Understanding the functional differences between isolates can be achieved through genetic screens using CRISPRi and transposon-sequencing (TnSeq) libraries. Typically, TnSeq and the subsequent identification of essential genes have been conducted in lab-adapted reference strains. However, in recent years, groups have performed TnSeq on clinical isolates of pathogens including *S. enterica, S.*

pneumoniae and *S. aureus.* All of these studies identified genes that were differentially essential among clinical isolates (19, 21–23). Notably, Carey *et al* performed TnSeq on 8 *Mtb* clinical isolates distributed across 3 lineages and discovered genes with differential requirements relative to the reference *Mtb* strain (24). Some of these genes were targets for antibiotics and the differences in genetic requirement correlated with antibiotic sensitivity. Carey *et al*'s study and others demonstrate that differences in genetic requirement among isolates do influence clinically relevant phenotypes.

For *Mab*, the majority of TnSeq studies published to date have used the lab-adapted reference strain, ATCC 19977 (25–27). One TnSeq study was conducted on a *massiliense* clinical isolate, however the transposon library was not dense enough to quantify genetic requirement (28). Currently, there are no published studies investigating the functional diversity of *Mab* clinical isolates. In order to do this, we conducted TnSeq on 22 *Mab* strains generating triplicate libraries for 15 *abscessus* isolates and 6 single libraries of the *massiliense* isolates. Across the 22 strains, we found that 562 genes, representing ~15% of the *Mab* core genome, were differentially required among isolates. We also identified genes whose differences in genetic requirements were sub-species, lineage, and isolate specific. Finally, we identified pairs of genes whose genetic requirements were correlated and thus unearthed previously undescribed genetic networks in *Mab*. Overall, we find that the genetic diversity present in *Mab* is matched with significant functional genomic diversity.

Results

Characterization of *Mab* clinical isolates

Twenty-five *Mab* isolates were collected from patients in Taiwan and locally at Brigham and Women's Hospital (BWH) (Supplementary Table 1). The clinical isolates were isolated from several body sites and passaged once to decrease selection of mutants under *in vitro* growth conditions. To determine the genetic diversity present in the clinical isolates, we performed whole genome sequencing (WGS), *de novo assembly* using ABySS (29), and annotated the genomes using RAST (see Methods). The average number of nucleotides in the assemblies was 5103719 bp. Summary statistics of the WGS data are presented in Supplementary Table 2. A phylogeny of the 25 clinical isolates and 5 reference strains based on genome-wide SNPs is shown in Figure 1A. To put these isolates into broader genomic context, they were incorporated into a global phylogeny constructed from 307 *Mab* strains from Bryant *et al* (11). The resulting tree recapitulated the three major subspecies of *Mab*, with our clinical isolates distributed across the entire tree (Figure 1B).

Analysis of *Mab* core and accessory genome content

We next identified the core and accessory genome content among the clinical isolates using the Ptolemy pan-genome analysis software program (30). From our panel of *Mab* clinical isolates, we identified 15,352 gene clusters representing distinct open reading frames (ORFs) (Supplemental Table S3). Of these, ~75% of the gene clusters were in the core genome defined as present in at least 95% of the 30 isolates. The remaining ~25% of gene clusters, or 11,507 ORFs, were in the accessory genome (Figure 2A). The genomes averaged ~5200 genes, with the number of accessory genes ranging from 997 genes in T52 to 1688 genes in BWH-E. On average, the core genome comprised 75.6% of the total gene content in each strain, while the accessory genome accounting for 24.4%. These values are consistent with results published from previous studies (13,31). As expected, isolates that were more distantly related to the reference ATCC 19977 strain generally shared less accessory genome content (Figure 2B). The diversity of the accessory genome was remarkable as evidenced by the number of isolates that contain distinct ORFs not present in any other isolates (Figure 2C). Of the 11,507 accessory genes identified, nearly 64% (n = 7361) were present in just 1 strain. The remaining 4147 genes were present in multiple (2-28)

isolates. Of these, 1114 were monophyletic genes meaning they were either inserted or deleted at one evolutionary time point and subsequently inherited by all the strains on that branch of the phylogenetic tree. The remaining 3210 accessory genes were polyphyletic. A subset of the monophyletic genes was sub-species specific and present in only *abscessus* or *massiliense* isolates (Figure 2D).

Transposon-sequencing of multiple *Mab* clinical isolates

Given the large genomic diversity present in *Mab*, we performed TnSeq across multiple clinical isolates to characterize the species' functional diversity. Specifically, we sought to identify genes that were differentially required among the isolates. We selected 22 isolates for TnSeq, and generated libraries in triplicate for 16 *abscessus* subsp. isolates and single replicate libraries for *6 massiliense* subsp. isolates. A schematic of the TnSeq experiment is presented in Supplemental Figure 1A. The transduction efficiency of the clinical isolates varied greatly, with the highest efficiencies observed in the two reference strains: ATCC 19977 and *massiliense* GO 06 (hereafter referred to as *massiliense*) (Supplemental Figure 1B). After transduction, >150,000 independent mutants were harvested from each replicate, and sequencing libraries were prepared for next-generation sequencing.

Sequencing revealed that the majority of our libraries were well saturated with a median of 59.5% of 'TA' dinucleotide sites containing a transposon insertion. This range of percent saturation spanned 20% to 70.3% (Supplemental Figure 1C). Libraries with less than 20% saturation were excluded from further analysis. The summary statistics for each library is presented in Supplementary Table 4**.** To assess the reproducibility of our replicates, we performed pairwise comparisons assessing the number of insertions in each gene between two replicate libraries for each strain. We found that the majority of the replicates were well correlated with a median Pearson r^2 value of 0.88 (Supplemental Table 5). The high degree of correlation between libraries and their high saturation gave us confidence that our libraries were of sufficient quality to use for further analyses.

HMM reveals essential genes in *Mab* clinical isolates

Using the Hidden Markov Model (HMM) algorithm (32), we determined the essentiality of each gene in the isolates' genomes. The genes were categorized as being either essential, non-essential, growth defect, or growth advantage. Genes classified as 'growth defect' are not technically essential, but their disruption causes growth impairment. Conversely, genes classified as 'growth advantage' cause a fitness benefit relative to wildtype when they are disrupted. The essential genes of the reference strain, ATCC 19977 have been previously reported (25,27). For the remaining clinical isolates, the essentiality call for each gene is listed in Supplemental Table 6. In total, the average number of essential genes across the clinical isolates was 386 genes with a range of 277 - 818. The number of non-essential genes varied significantly among strains, ranging from 3137 - 4172 (Supplemental Figure 2). The combined number of essential and growth-defect genes (avg ~468) is consistent with essentiality analyses of other mycobacteria, where essential genes typically represent 10-15% of the genome (33,34).

ANOVA identifies additional differentially required genes

Traditionally, the 'resampling' method from TRANSIT is used to identify differentially required genes between two strains (32). We performed resampling between each clinical isolate and the reference ATCC 19977 strain, and the summary of these analyses are in Supplemental Table 7. While resampling is a powerful analytical tool, it limits our analyses to identifying differences in gene requirement between only two strains at a time. To compare the transposon insertion counts across all strains simultaneously, we used ANOVA. For this analysis, we included all the genes in the core genome, as well as genes in the pan-genome that appeared in at least 5 isolates. ANOVA identified 562 genes that were differentially required across all 22 clinical isolates (Supplemental Table 8). For each gene, the log2-fold-change (LFC) of the insertion counts in each isolate was calculated relative to the grand mean across all isolates. These LFCs are depicted in a heatmap (Figure 3). Hierarchical clustering of the isolates revealed that the *massiliense* isolates (T36, T49, T52, BWH-D, BWH-F, *massiliense*) group together. Interestingly, isolates T37, T40, T44, and Bamboo cluster with the *abscessus* sub-species isolates by SNP data (Figure 1B); however, by TnSeq data, they cluster with each other and apart the other *abscessus* sub-species strains (Figure 3). Thus, our TnSeq data highlights a discrepancy between the phylogenetic relationship of strains via SNP differences versus their functional relationship via transposon insertion differences.

The 562 genes identified by ANOVA as differentially required represent ~15% of the *Mab* core genome. Furthermore, 484 of these genes are non-essential in the reference ATCC 19977 genome (Figure 3B). These data reinforce the concept that genes can be differentially required based on environmental condition and genetic background (24).

Gene essentiality varies by lineage and by strain

To better understand the variance in the ANOVA data set, we used principal component analysis (PCA) to group the hit genes. The analysis showed principal components (PC) 1 & 2 explain ~40% of the variation in the data (Figure 4A). When the isolates are clustered into 3 groups, they do so primarily by phylogenetic relationship, where cluster 1 is a sub-lineage of the *abscessus* subspecies, cluster 2 has the *abscessus* sub-species that are more closely related to the reference ATCC 19977 strain, and cluster 3 contains the *massiliense* subspecies. PCs 1 and 2 represent lineage-specific differences in gene requirement, while when PCs 3 and 4 are plotted, the phylogenetic clustering collapses (Figure 4B). The phylogenetic tree from Figure 1B is color coded with the respective three clusters and demonstrates that closely related isolates share genetic requirements and suggests a shared evolutionary origin to how these differences arise.

The variation in PCs 1 and 2 only explain ~40% of the variation in the dataset, corresponding to lineage-specific variation. In contrast, PCs 3-19 explain the remaining ~60% of the variation and likely represents strain-specific variation or noise (Figure 4D). The top 10 genes that contribute to the variance in PCs 1 and 2 are plotted in Figure 7E. The genes in PC 1 separate the two subspecies, while the genes in PC 2 separate Cluster 1 strains (T35, T37, T50, and T56) from the rest of the clinical isolates (Figure 4E).

Identification of genes with lineage-specific essentiality

We next examined genes that exhibited lineage-specific differences in genetic requirement. We first identified genes that separated the clinical isolates from the reference strain in the PCA. Two genes in particular were the strongest differentiators: *MAB_4502c*, which encodes phosphoenolpyruvate

carboxykinase (*pckA*), and *MAB_1327,* which encodes ferredoxin *(fdxC*) (Figure 5A). The reference strain has quantitatively less of a requirement for *pckA* than the clinical isolates. This difference could be due to lab adaptation of the reference strain, a hypothesis we explore in the Discussion.

We next analyzed the contributing genes in PC 1 that separate the two sub-species of *Mab abscessus* vs. *massiliense.* The top 4 genes are depicted in Figure 5B, while the top 20 genes that separate the two subspecies are listed in Supplementary Table 9. We next inspected genes that separated strains in Cluster 1 (T35, T37, T50, and T56) from the rest of the clinical isolates (Figure 5C). The top 20 genes that contribute to the variation in this cluster are listed in Supplementary Table 10. Future work is needed to understand what the functional consequences of these differences are and whether they confer sub-species specific phenotypes with clinical relevance.

The genes that are uniquely required in Cluster 1 can be split into three groups depending on how many strains share the level of requirement. For group 1, all four strains in the cluster have the same strong requirement for 3 genes in an operon, *MAB_2724c-MAB_2726c* (hypothetical genes of unknown function). Group 2 genes are shared only by T35, T37, and T56, which are more related to each other than T50. Finally, group 3 is composed of genes shared by the two most closely related strains, T35 and T56. These data reveal genetic requirement emerging within a lineage. As strains diverge, their genomes not only change in genetic sequence, but also in function, and genes that are otherwise dispensable in one strain can become more required in another. This is best illustrated by genes *MAB_4950c* and *MAB_1055c*, which are most strongly required in the two isolates that are phylogenetically the most related, T35 and T56.

Correlated transposon insertion counts reveal functional genetic networks

In order to extract functional inferences from our TnSeq dataset, we looked for pairs of genes with correlated transposon insertion counts, which could potentially reveal hidden functional genetic networks. To conduct this analysis, we selected the 751 unique ORFs with the most variability based on ANOVA (P adj < 0.05) and other filters (see Methods). Of the total 282,000 potential gene pairings, only 10,198 were

significantly correlated, representing 3.6% of total potential pairs (Supplemental Table 11). In Figure 6A, we show 3 examples of gene pairs that are positively correlated with each other. Pair 1 are genes *MAB_2725c x MAB_2726c*, whose insertion counts across all 22 clinical isolates were correlated with an r^2 of 0.92. The next two pairs, *MAB_2725c x MAB_3333*, and *MAB_3246c x MAB_3333* also have statistically significant correlated insertions counts. In fact, all these genes are correlated with each other.

Based on these pairwise gene correlations, we performed network analysis with Cytoscape to turn these pairwise correlations into a network of interconnected genes. The network was organized into 19 clusters based on a greedy community identification algorithm (see Methods), so that related genes with similar transposon insertion profiles were clustered together. This analysis identified 19 clusters each containing at least 5 genes. The genes profiled in Figure 7A are members of cluster 7 and are labeled in the network (Figure 6B). Cluster 7 is comprised of 13 genes and includes the previously highlighted operon *MAB_2724c – MAB_2726* as well as 10 other genes including *ruvA* and *ruvB*, which both encode Holliday junction ATP-dependent DNA helicases, and *MAB_3246c*, which encodes *smc*, segregation and condensation protein (Figure 6B).

The full network analysis with a few of the clusters highlighted are depicted in Figure 6C. The full list of clusters extracted by our analysis is provided in Supplemental Table 12. These genetic networks could only be revealed by TnSeq and comparative analysis across multiple genetically-diverse strains. Future work can validate these networks, interrogate the functional consequence of perturbing them, and generate new insights into *Mab* physiology.

Genes involved in central carbon metabolism are differentially required among clinical isolates

Resampling analysis unveiled several differentially required genes involved in carbon metabolism among the clinical isolates and reference strain (Figure 7A). As noted above, *pckA* is more required in clinical isolates than in ATCC 19977. Other examples include *mqo* (malate:quinone oxidoreductase), which is most required in T50 and BWH-F and *pgi* (glucose-6-phosphate isomerase), which is most required in T35 and T56. In order to validate these differences, we employed CRISPRi/Cas9 methodology to repress

pckA, which is more required in all the clinical isolates except ATCC 19977, BWH-B, BWH-C, and T45. We found that when *pckA* is repressed in ATCC 19977, there was no difference in CFUs between induction and non-induction plates as predicted by the plate data (Figure 7B). However, when we repressed the enzyme in T35, T50, and T56 we observed a 10X to 100X decrease in CFUs, indicating that *pckA* is indeed more required in these clinical isolates. In contrast, when we repressed *pckA* in T45 and BWH-B there was no difference in CFUs, further corroborating the TnSeq data that *pckA* is less required in these isolates.

We also repressed *sdhB*, which was predicted to be required in ATCC 19977 and less required in the T49. Repressing *sdhB* in ATCC 19977 led to a 100X fold decrease in CFUs. However, when *sdhB* was repressed in T49, there was no difference in CFUs, confirming that *sdhB* is less required in T49. These knockdown experiments validate our genetic requirement data and corroborate the functional differences in carbon metabolism between the clinical isolates.

Discussion

While several groups have described the genomic diversity of *Mab* clinical isolates (13,16,17), to date there have been no studies interrogating the functional consequence of this diversity. To investigate the functional diversity and genetic requirements of *Mab*, we performed TnSeq on 22 *Mab* clinical isolates spanning both the *abscessus* and *massiliense* sub-species. Among the 22 isolates, we identified 562 genes or ~15% of the *Mab* core genome as being differentially required among the isolates. This includes genes that were non-essential in the reference strain and became either fully essential or more required in some clinical isolates. This latter case highlights the concept of "vulnerability" in gene essentiality studies. First defined by Bosch *et al* who demonstrated that repression of essential genes does not lead to equivalent reductions in fitness (35). More 'vulnerable' essential genes yield larger reductions in fitness when repressed as compared to less vulnerable genes (35). Our data expands on this concept by demonstrating non-essential genes similarly have varying levels of vulnerability.

Applying TnSeq to a genetically diverse group of isolates enabled us to uncover functional differences among core and accessory genes. Using PCA and network analysis, we identified significant clusters of genes whose insertion patterns were correlated, and for which functional requirements varied with phylogenetic position, including genes whose differences in genetic requirement were subspecies-specific. This data implied that *Mab* subspecies have evolved to require a distinct subset of genes. Given that our experiment was conducted under *in vitro* laboratory conditions, passaging our transposon mutant libraries through more environmental or disease-related conditions might reveal additional variability in genetic requirement. Recently, Sullivan *et al* passaged a transposon mutant library of clinical isolate T35 on an *in vitro* lung model and identified key metabolic genes responsible for establishing lung infection (36). Future such studies testing more isolates in varied conditions will uncover new and clinically relevant genetic requirements in *Mab.*

We also identified differences in gene requirement that were lineage-specific. Strains T35, T37, T50, and T56 represent one distinct lineage of the *abscessus* sub-species with genetic requirements that were unique to these strains. Notably, the operon *MAB_2724c-MAB_2726c* was uniquely required in this

lineage and contributed 20% of the variance separating this sub-lineage from all the other clinical isolates. All three genes in the operon are annotated as hypothetical proteins, and future studies are needed to understand why this operon is uniquely required in this subset of strains. Furthermore, within this lineage of four strains, we also observed step-wise development of gene requirement, highlighting that gene essentiality is not static, but rather can emerge and evolve over time (Figure 5C).

Interestingly, our study identified functional differences between the reference strain and the clinical isolates in genes related to carbon metabolism. Specifically, the gene *MAB_4502c* encodes the enzyme phosphoenolpyruvate carboxykinase, *pckA*, and is more required in nearly all of the clinical isolates compared to the reference strain. *pckA* catalyzes the conversion of oxaloacetate to phosphoenolpyruvate, which is the first committed step of gluconeogenesis. The reduced requirement for *pckA* in ATCC 19977 is likely a consequence of the adaptation of the reference strain to being passaged on rich media with ample sources of carbon for 70+ years (37). Thus, the reference strain may have evolved to be less dependent on gluconeogenesis as an energy source.

An open question raised by this study is what role the accessory genome plays in driving variability in genetic requirements among *Mab* strains. *Mab* is well-known to have a large accessory genome, which we confirmed using pan-genome analysis. Gene acquisition and gene loss through mechanisms such as plasmid transfer, phage integration, duplication, or large-scale deletion, likely influences genetic requirement and functional differences between strains. More work is needed to untangle the effects of the presence and absence of these accessory genes on essentiality of genes in the *Mab* core genome.

In summary, this study is the first to demonstrate that there are functional genomic differences among *Mab* clinical isolates, which could provide additional insights into understanding and eventually better treating this emerging pathogen.

Methods

Bacterial strains and culture conditions: *Mab* clinical strains were isolated from patients in Taiwan (T) and Brigham and Women's Hospital (BWH), Boston, MA. Clinical isolates were streaked from patient stabs, single colonies were picked, cultured, and frozen for future use. Strains with transformed CRISPRi/Cas9 vectors to knockdown central carbon metabolism genes were built as described in (27). All strains were grown shaking at 37°C in liquid 7H9 media consisting of Middlebrook 7H9 salts with 0.2% glycerol, 0.85 g/L NaCl, and OADC (oleic acid, 5 g/L albumin, 2 g/L dextrose, 0.003 g/L catalase), and 0.05% Tween80. All *Mab* strains were plated on Middlebrook 7H10 agar supplemented with 10% OADC and 0.05% Tween80. Kanamycin 100 µg/ml was used for selection. Induction of all CRISPRi/Cas9 plasmids was performed with 500 ng/µl ATc.

Whole Genome Sequencing of *Mab* Clinical Isolates: Genomic DNA from late-log phase cultures were extracted via a bead-beating and phenol-chloroform protocol described in Akusobi *et al* (27). DNA samples were then sheared to a size range of 200-400 bp using sonication with Covaris tubes. Afterwards, samples were prepared using Illumina TruSeq sample-prep kits with adapters for multiplexing. The samples were then sequenced on an Illumina Rapid HiSeq 2500 instrument with 125+125 bp paired-end reads.

Genome Assembly: Genome sequences for each isolate were assembled *de novo* from .fastq files using ABySS (v2.0) with default parameters (29). The assemblies typically contained 50-100 contigs sized >1kb, with a mean N50 of 204kb (range: 133-288kb) and mean total length of 5.14 Mbp (range: 4.86-5.54Mb) (Supplemental Table 2). To assemble core genomes (files labeled as sync3), the contigs were mapped onto the *M. abscessus* ATCC 19977 (NC_010397.1) reference genome using Blastn, and then concatenated in syntenic order. When possible, gaps between contigs were patched by local contig building using the overlap-consensus method (38). Final genome length and depth of coverage are shown in Supplemental Table 2. To distinguish among *Mab* subspecies, the pattern of nucleotide substitutions was examined in *hsp65/groEL2* (39).

Genome Alignment and Annotation: Genome alignments were made using MUMMER v3.23 to identify exact-matching regions (40). To identify SNPs and indels, regions with genetic variation were aligned using the Needleman-Wunsch algorithm (41). For core genomes, the coordinates of open reading frames (ORFs) were adjusted for each isolate using a whole-genome alignment to the reference genome. Genes where the start or end coordinates were deleted in a clinical isolate likely represented a deleted gene and were removed from the annotation. These adapted annotations are provided as files labeled ".mabs_mod.prot_table". To produce unbiased annotations of each clinical isolate, we also ran RAST (PATRIC CLI v1.039) on the contigs generated by ABySS (42). These annotations contain all predicted ORFs on all contigs, including those on plasmids and large insertions not found in the reference strain.

Phylogenetic Analysis: To construct a phylogenetic tree incorporating all the *Mab* clinical isolates and reference strains, an alignment of all the core genomes was first generated. The included reference strains were: *M. abscessus* ATCC 19977 (NC_010397.1), *M. abscessus* subsp. massiliense CCUG 49989 (NZ_AHAR01000001.1) and GO 06 (NC_018150.2), *M. abscessus* subsp. bolletii FLAC003 (CP014950.1), and two additional *M. abscessus* subsp. abscessus clinical isolates from Taiwan: *M. abscessus* str. bamboo (NZ_MVDX00000000.1) and *M. abscessus* str. K21 (sequencing data were kindly provided by M. Gengenbacher). For all isolates, regions with insertions or deletions were filtered out, along with sites exhibiting low-coverage (<10x), heterogeneity (<70% base-call purity) or repetition (where an overlapping window of 35 bp matches with at least 33/35 bp elsewhere in the genome). Finally, the remaining list of SNPs was extracted and used as input to *dnapars* in Phylip 3.66 (43) to generate the maximum parsimony phylogenetic tree, rooted using *M. chelonae* str. CCUG 47445 (NZ_CP007220.1) as an outgroup. A larger tree expanded with 306 additional *Mab* isolates from a study by Bryant *et al* (11) was generated using TNT (44).

Pan-Genome Analysis: The pan-genome analysis was performed using Ptolemy v1.0 (30) to determine mappings of orthologs among ORFs based on both homology and synteny. ABySS assemblies (contigs) were used as input for each isolate, along with the ORFs from the RAST annotation (converted to .gff format). Post-processing of the "orf2node_id.txt" output files was used to generate a spreadsheet with all

“pan-ORFs” (15,352 ortholog clusters) as rows and individual ORF ids in columns. This data is provided in Supplemental Table 3. This file also contains a count of how many of the 30 strains had a copy of each pan-ORF, which was used to differentiate core genes (genes with orthologs in >95% of isolates) from accessory genes (present in 1-28 isolates). For accessory genes, the subset of isolates containing them was mapped onto the phylogenetic tree to determine: monophyletic, polyphyletic, and subspecies-specific genes.

Generation of *Mab* Clinical Isolate Libraries: High-density transposon libraries of *Mab* clinical isolates were generated using the ϕMycoMarT7 phage as described in Akusobi *et al* (27). Libraries were generated in biological triplicate for 15 clinical isolates (ATCC 19977, T35, T37, T40, T45, T49, T50, T51, T53, T55, T56, BWH-B, BWH-C, BWH-E, BWH-F), while single replicate libraries were generated for 6 isolates (T36, T52, BWH-H, *M. abscessus subsp. massiliense* CCUG 48898 (AHAR01000001.1), K21 (a generous gift from Thomas Dick, Meridian Health, Hackensack, NJ), and Bamboo (MVDX01000001.1). Libraries were selected for 4 days on 7H10 agar supplemented with 10% OADC, 0.5% glycerol, 0.05% Tween80 and kanamycin 100 µg/ml. Libraries of >150,000 mutants were harvested and stored in 7H9 + 10% glycerol in -80°C for future use. Transposon-sequencing libraries were prepared following the protocol described in (45). The TnSeq samples were also sequenced on an Illumina Rapid HiSeq 2500 instrument with 125+125 bp paired-end reads.

TnSeq Analysis: The .fastq files obtained from sequencing were pre-processed using TPP in Transit (32). The reads were then mapped to the syntenic versions of each genome (aligned to ATCC 19977), and the raw Abyss assemblies (all contigs) of each isolate. The median library saturation was 58.4% (range: 19.0-72.6%) (Supplementary Table 4). BWH-B-2 and BWH-C-1 were excluded from further analyses due to low saturation and poor skew, respectively.

To identify essential and non-essential genes in each isolate, the Hidden Markov Model (HMM) in Transit was run (Supplemental Table 6). To identify conditionally essential genes in each isolate relative to ATCC 19977, the ‘resampling’ method in Transit was used. Resampling compares the mean insertion count in

each gene (pooled over TA sites and replicates) to a null distribution between 2 strains. P-values are adjusted for multiple tests by the Benjamini-Hochberg procedure (46) for an FDR of 5%. Significant genes are those with P-adj < 0.05 (Supplemental Table 7). To identify genes with significant variability of insertion counts across strains, ANOVA analysis was applied to the pan-ORFs. The normalized counts at each TA site for each gene were tabulated and averaged at the strain level. Then one-way ANOVA was used to calculate the F-statistic and P-value, where were adjusted by the Benjamini-Hochberg procedure for an FDR of 5%.

Genetic Interactions and Network Analysis: A correlation analysis of mean transposon insertion counts was performed for gene pairs across all *Mab* strains. Genes with significant variability by ANOVA (P-adj < 0.05) and insertion count < 20 or Z-max > 8 (used to filter out outliers) were selected resulting in 751 varying genes. For gene pairs that were jointly present in at least 10 strains, a Pearson correlation coefficient was calculated. This analysis identified 10,198 pairs of genes with a correlation of > 0.7 and adjusted p-value < 0.05. A network diagram based on these correlations was generated in Cytoscape v3.9.1 using the Edge-weighted Spring-embedded Layout.

To extract clusters of genes with similar TnSeq profiles, a network community analysis was performed based on a greedy algorithm. The degree of each gene was calculated, reflecting the number genes correlated to it with cc > 0.7. The gene with the highest degree represented the most “central” gene in the network, and was required to be present in at least 15 strains. We extracted the cluster of genes connected to the most central gene as the first cluster. To extract subsequent clusters, we identified the next most central gene whose neighbors did not overlap more than 20% with genes in previously selected clusters. The process was iterated until clusters contained fewer than 5 genes.

References

1. Baldwin SL, Larsen SE, Ordway D, Cassell G, Coler RN. The complexities and challenges of preventing and treating nontuberculous mycobacterial diseases. PLoS Negl Trop Dis. 2019 Feb 14;13(2):e0007083.

2. Adjemian J, Olivier KN, Seitz AE, Falkinham JO, Holland SM, Prevots DR. Spatial clusters of nontuberculous mycobacterial lung disease in the United States. Am J Respir Crit Care Med. 2012 Sep 15;186(6):553–8.

3. Lee MR, Sheng WH, Hung CC, Yu CJ, Lee LN, Hsueh PR. Mycobacterium abscessus Complex Infections in Humans. Emerg Infect Dis. 2015 Sep;21(9):1638–46.

4. Nessar R, Cambau E, Reyrat JM, Murray A, Gicquel B. Mycobacterium abscessus: a new antibiotic nightmare. J Antimicrob Chemother. 2012 Apr;67(4):810–8.

5. Pang H, Li G, Wan L, Jiang Y, Liu H, Zhao X, et al. In vitro drug susceptibility of 40 international reference rapidly growing mycobacteria to 20 antimicrobial agents. Int J Clin Exp Med. 2015;8(9):15423–31.

6. Nash KA, Brown-Elliott BA, Wallace RJ. A Novel Gene, erm(41), Confers Inducible Macrolide Resistance to Clinical Isolates of Mycobacterium abscessus but Is Absent from Mycobacterium chelonae. Antimicrob Agents Chemother. 2009 Apr;53(4):1367–76.

7. Hurst-Hess K, Rudra P, Ghosh P. Mycobacterium abscessus WhiB7 Regulates a Species-Specific Repertoire of Genes To Confer Extreme Antibiotic Resistance. Antimicrob Agents Chemother. 2017 Oct 24;61(11):e01347-17.

8. Koh WJ, Stout JE, Yew WW. Advances in the management of pulmonary disease due to Mycobacterium abscessus complex. Int J Tuberc Lung Dis Off J Int Union Tuberc Lung Dis. 2014 Oct;18(10):1141–8.

9. Koh WJ, Jeong BH, Kim SY, Jeon K, Park KU, Jhun BW, et al. Mycobacterial Characteristics and Treatment Outcomes in Mycobacterium abscessus Lung Disease. Clin Infect Dis Off Publ Infect Dis Soc Am. 2017 Feb 1;64(3):309–16.

10. Tortoli E, Kohl TA, Brown-Elliott BA, Trovato A, Leão SC, Garcia MJ, et al. Emended description of Mycobacterium abscessus, Mycobacterium abscessus subsp. abscessus and Mycobacteriumabscessus subsp. bolletii and designation of Mycobacteriumabscessus subsp. massiliense comb. nov. Int J Syst Evol Microbiol. 2016 Nov;66(11):4471–9.

11. Bryant JM, Grogono DM, Rodriguez-Rincon D, Everall I, Brown KP, Moreno P, et al. Emergence and spread of a human-transmissible multidrug-resistant nontuberculous mycobacterium. Science. 2016 Nov 11;354(6313):751–7.

12. Wee WY, Dutta A, Choo SW. Comparative genome analyses of mycobacteria give better insights into their evolution. PLOS ONE. 2017 Mar 14;12(3):e0172831.

13. Choo SW, Wee WY, Ngeow YF, Mitchell W, Tan JL, Wong GJ, et al. Genomic reconnaissance of clinical isolates of emerging human pathogen Mycobacterium abscessus reveals high evolutionary potential. Sci Rep. 2014 Feb 11;4(1):4061.

14. Ripoll F, Pasek S, Schenowitz C, Dossat C, Barbe V, Rottman M, et al. Non mycobacterial virulence genes in the genome of the emerging pathogen Mycobacterium abscessus. PloS One. 2009 Jun 19;4(6):e5660.

15. Gagneux S. Ecology and evolution of Mycobacterium tuberculosis. Nat Rev Microbiol. 2018;16(4):202–13.

16. Sapriel G, Konjek J, Orgeur M, Bouri L, Frézal L, Roux AL, et al. Genome-wide mosaicism within Mycobacterium abscessus: evolutionary and epidemiological implications. BMC Genomics. 2016 Feb 17;17:118.

17. Tan JL, Ng KP, Ong CS, Ngeow YF. Genomic Comparisons Reveal Microevolutionary Differences in Mycobacterium abscessus Subspecies. Front Microbiol. 2017;8:2042.

18. Brockhurst MA, Harrison E, Hall JPJ, Richards T, McNally A, MacLean C. The Ecology and Evolution of Pangenomes. Curr Biol. 2019 Oct 21;29(20):R1094–103.

19. Rosconi F, Rudmann E, Li J, Surujon D, Anthony J, Frank M, et al. A bacterial pan-genome makes gene essentiality strain-dependent and evolvable. Nat Microbiol. 2022 Oct;7(10):1580–92.

20. Rousset F, Cabezas-Caballero J, Piastra-Facon F, Fernández-Rodríguez J, Clermont O, Denamur E, et al. The impact of genetic diversity on gene essentiality within the Escherichia coli species. Nat Microbiol. 2021 Mar;6(3):301–12.

21. Opijnen T van, Dedrick S, Bento J. Strain Dependent Genetic Networks for Antibiotic-Sensitivity in a Bacterial Pathogen with a Large Pan-Genome. PLOS Pathog. 2016 Sep 8;12(9):e1005869.

22. Coe KA, Lee W, Stone MC, Komazin-Meredith G, Meredith TC, Grad YH, et al. Multi-strain Tn-Seq reveals common daptomycin resistance determinants in Staphylococcus aureus. Peschel A, editor. PLOS Pathog. 2019 Nov 18;15(11):e1007862.

23. Karlinsey JE, Stepien TA, Mayho M, Singletary LA, Bingham-Ramos LK, Brehm MA, et al. Genome-wide Analysis of Salmonella enterica serovar Typhi in Humanized Mice Reveals Key Virulence Features. Cell Host Microbe. 2019 Sep 11;26(3):426-434.e6.

24. Allison F. Carey, Rock JM, Krieger IV, Chase MR, Fernandez-Suarez M, Gagneux S, et al. TnSeq of Mycobacterium tuberculosis clinical isolates reveals strain-specific antibiotic liabilities. PLOS Pathog. 2018 Mar 5;14(3):e1006939.

25. Rifat D, Chen L, Kreiswirth BN, Nuermberger EL. Genome-Wide Essentiality Analysis of Mycobacterium abscessus by Saturated Transposon Mutagenesis and Deep Sequencing. mBio. 2021 Jun 15;e0104921.

26. Foreman M, Gershoni M, Barkan D. A Simplified and Efficient Method for Himar-1 Transposon Sequencing in Bacteria, Demonstrated by Creation and Analysis of a Saturated Transposon-Mutant Library in Mycobacterium abscessus. mSystems. 2020 Oct 20;5(5):e00976-20.

27. Akusobi C, Benghomari BS, Zhu J, Wolf ID, Singhvi S, Dulberger CL, et al. Transposon mutagenesis in Mycobacterium abscessus identifies an essential penicillin-binding protein involved in septal peptidoglycan synthesis and antibiotic sensitivity. eLife. 2022 Jun 6;11:e71947.

28. Laencina L, Dubois V, Le Moigne V, Viljoen A, Majlessi L, Pritchard J, et al. Identification of genes required for Mycobacterium abscessus growth in vivo with a prominent role of the ESX-4 locus. Proc Natl Acad Sci U S A. 2018 30;115(5):E1002–11.

29. Jackman SD, Vandervalk BP, Mohamadi H, Chu J, Yeo S, Hammond SA, et al. ABySS 2.0: resource-efficient assembly of large genomes using a Bloom filter. Genome Res. 2017 May;27(5):768–77.

30. Salazar AN, Abeel T. Approximate, simultaneous comparison of microbial genome architectures via syntenic anchoring of quiver representations. Bioinformatics. 2018 Sep 1;34(17):i732–42.

31. Davidson RM. A Closer Look at the Genomic Variation of Geographically Diverse Mycobacterium abscessus Clones That Cause Human Infection and Disease. Front Microbiol. 2018;9:2988.

32. DeJesus MA, Ambadipudi C, Baker R, Sassetti C, Ioerger TR. TRANSIT--A Software Tool for Himar1 TnSeq Analysis. PLoS Comput Biol. 2015 Oct;11(10):e1004401.

33. Sassetti CM, Boyd DH, Rubin EJ. Genes required for mycobacterial growth defined by high density mutagenesis. Mol Microbiol. 2003 Apr;48(1):77–84.

34. DeJesus MA, Gerrick ER, Xu W, Park SW, Long JE, Boutte CC, et al. Comprehensive Essentiality Analysis of the Mycobacterium tuberculosis Genome via Saturating Transposon Mutagenesis. mBio. 2017 Jan 17;8(1):e02133-16.

35. Bosch B, DeJesus MA, Poulton NC, Zhang W, Engelhart CA, Zaveri A, et al. Genome-wide gene expression tuning reveals diverse vulnerabilities of M. tuberculosis. Cell. 2021 Aug 19;184(17):4579-4592.e24.

36. Sullivan MR, McGowen K, Liu Q, Akusobi C, Young DC, Mayfield JA, et al. Biotin-dependent cell envelope remodelling is required for Mycobacterium abscessus survival in lung infection. Nat Microbiol. 2023 Jan 19;1–17.

37. Moore M, Frerichs JB. An unusual acid-fast infection of the knee with subcutaneous, abscess-like lesions of the gluteal region; report of a case with a study of the organism, Mycobacterium abscessus, n. sp. J Invest Dermatol. 1953 Feb;20(2):133–69.

38. Li Z, Chen Y, Mu D, Yuan J, Shi Y, Zhang H, et al. Comparison of the two major classes of assembly algorithms: overlap–layout–consensus and de-bruijn-graph. Brief Funct Genomics. 2012 Jan 1;11(1):25–37.

39. Nakanaga K, Sekizuka T, Fukano H, Sakakibara Y, Takeuchi F, Wada S, et al. Discrimination of Mycobacterium abscessus subsp. massiliense from Mycobacterium abscessus subsp. abscessus in Clinical Isolates by Multiplex PCR. J Clin Microbiol. 2014 Jan;52(1):251–9.

40. Kurtz S, Phillippy A, Delcher AL, Smoot M, Shumway M, Antonescu C, et al. Versatile and open software for comparing large genomes. Genome Biol. 2004;9.

41. Needleman SB, Wunsch CD. A general method applicable to the search for similarities in the amino acid sequence of two proteins. J Mol Biol. 1970 Mar 28;48(3):443–53.

42. Brettin T, Davis JJ, Disz T, Edwards RA, Gerdes S, Olsen GJ, et al. RASTtk: a modular and extensible implementation of the RAST algorithm for building custom annotation pipelines and annotating batches of genomes. Sci Rep. 2015 Feb 10;5:8365.

43. Baum BR. PHYLIP: Phylogeny Inference Package. Version 3.2. Joel Felsenstein. Q Rev Biol. 1989 Dec 1;64(4):539–41.

44. Goloboff PA, Farris JS, Nixon KC. TNT, a free program for phylogenetic analysis. Cladistics. 2008;24(5):774–86.

45. Long JE, DeJesus M, Ward D, Baker RE, Ioerger T, Sassetti CM. Identifying essential genes in Mycobacterium tuberculosis by global phenotypic profiling. Methods Mol Biol Clifton NJ. 2015;1279:79–95.

46. Benjamini Y, Hochberg Y. Controlling the False Discovery Rate: A Practical and Powerful Approach to Multiple Testing. J R Stat Soc Ser B Methodol. 1995;57(1):289–300.

Figures and Legends

A

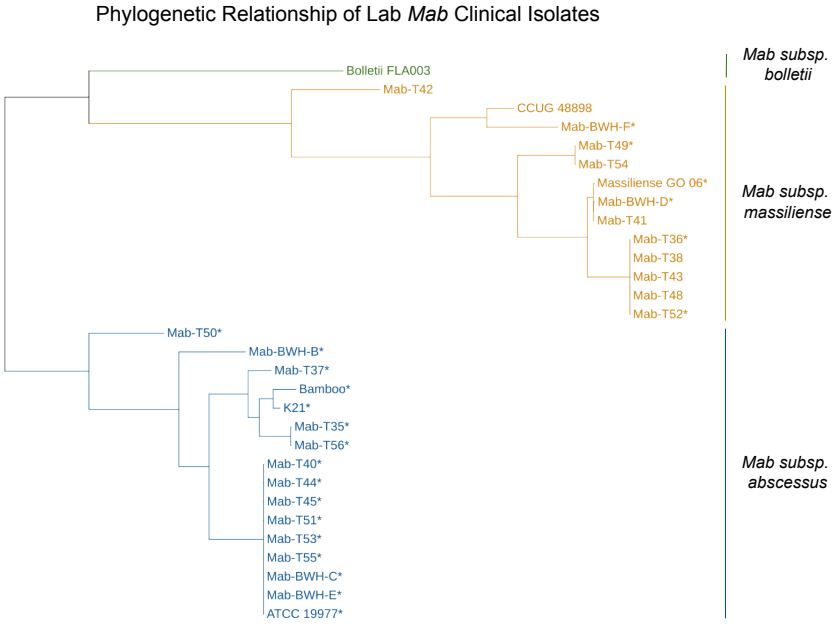

B

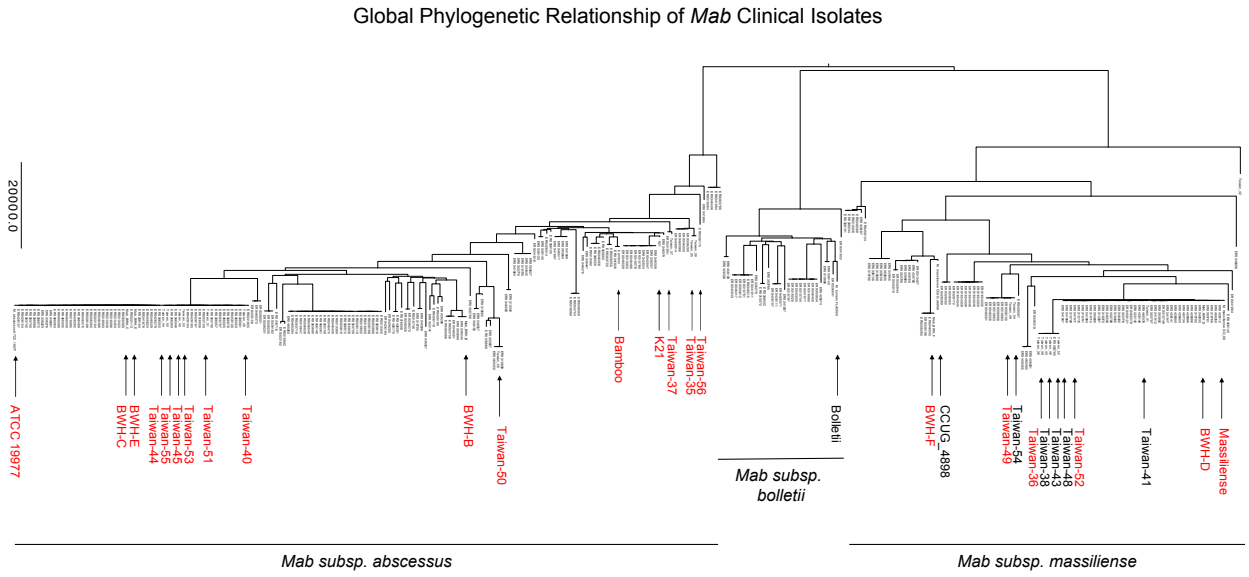

Figure 1: Phylogenetic Relationship of *Mab* Clinical Isolates. (A) Phylogenetic tree of 25 Mab clinical isolates and 5 reference strains. Strains with transposon mutant libraries are marked with an '*' **(B)** Global phylogenetic tree of *Mab* clinical isolates using genomes of 307 clinical isolates from Bryant *et al*, 2016. Strains in the lab are labeled with an arrow. Red arrows indicate strains that have transposon-mutant libraries

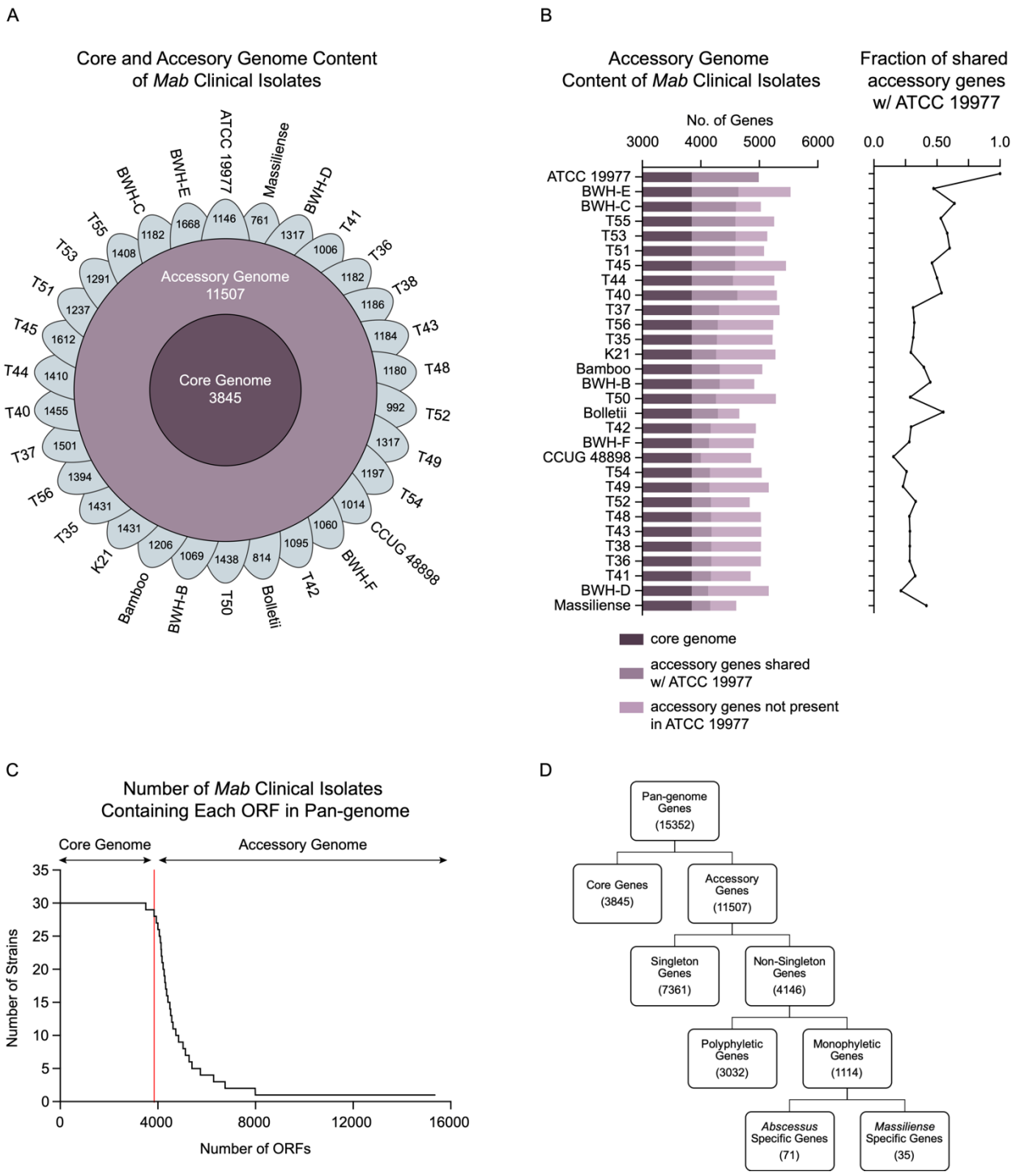

Figure 2: *Mab* has a large accessory genome. **(A)** Flower pot diagram showing the breakdown of core and accessory genes in lab *Mab* clinical isolates. The outer leaflets show the number of accessory genes present in each clinical isolate. Strains are arranged counterclockwise based on degree of similarity to the reference strain by core genome. **(B)** (*left*) Breakdown of accessory genome content in each clinical isolate. (*right*) Percentage of accessory gene content shared by the reference strain. **(C)** Number of ORFs present in the clinical isolates **(D)** Categorization of ORFs in the pan-genome

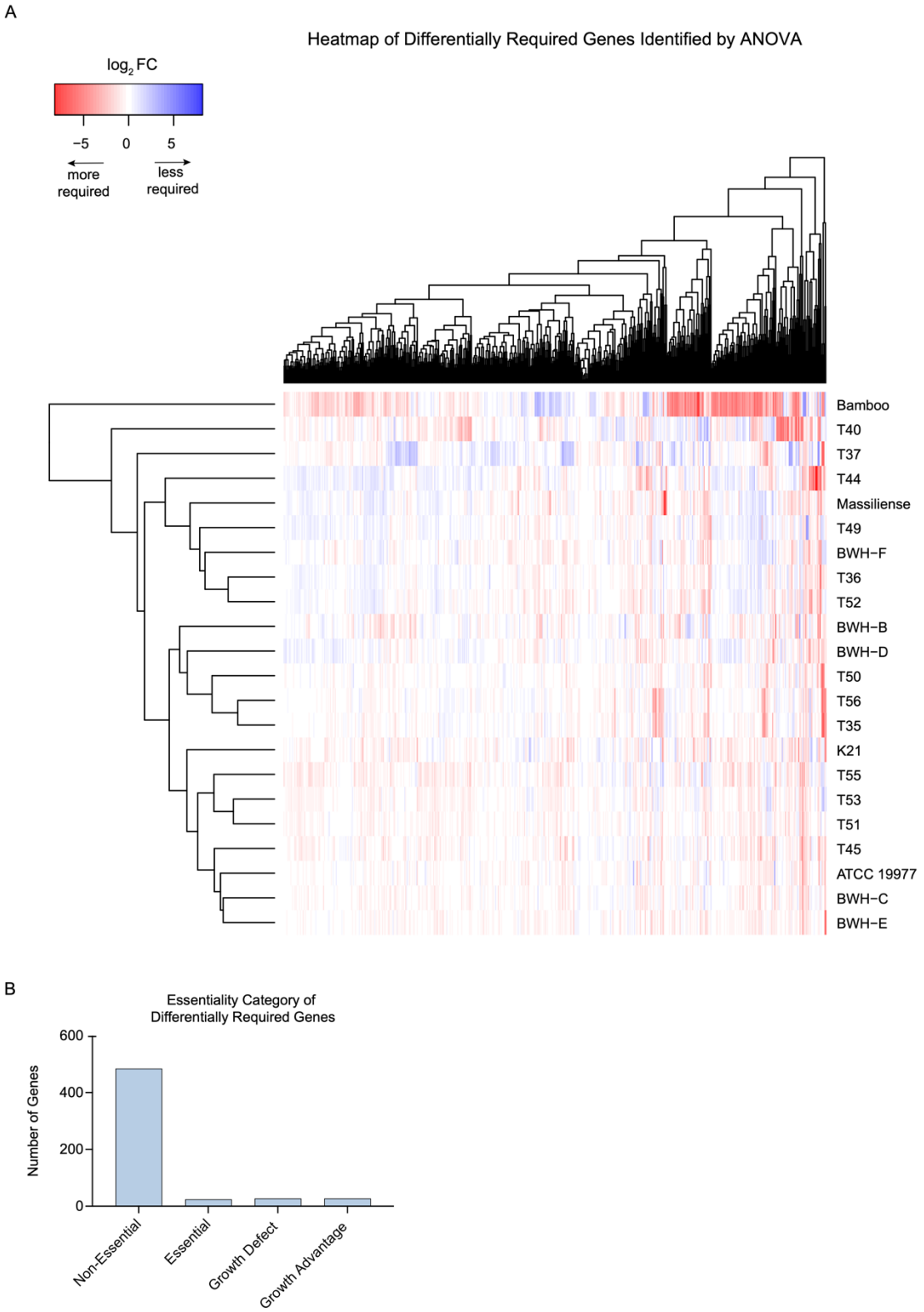

Figure 3: Summary of ANOVA results. (A) Heatmap depicting the LFCs of insertion counts for the 562 differentially required genes present in all isolates **(B)** Essentiality of the differentially essential genes in the ATCC 19977 reference strain

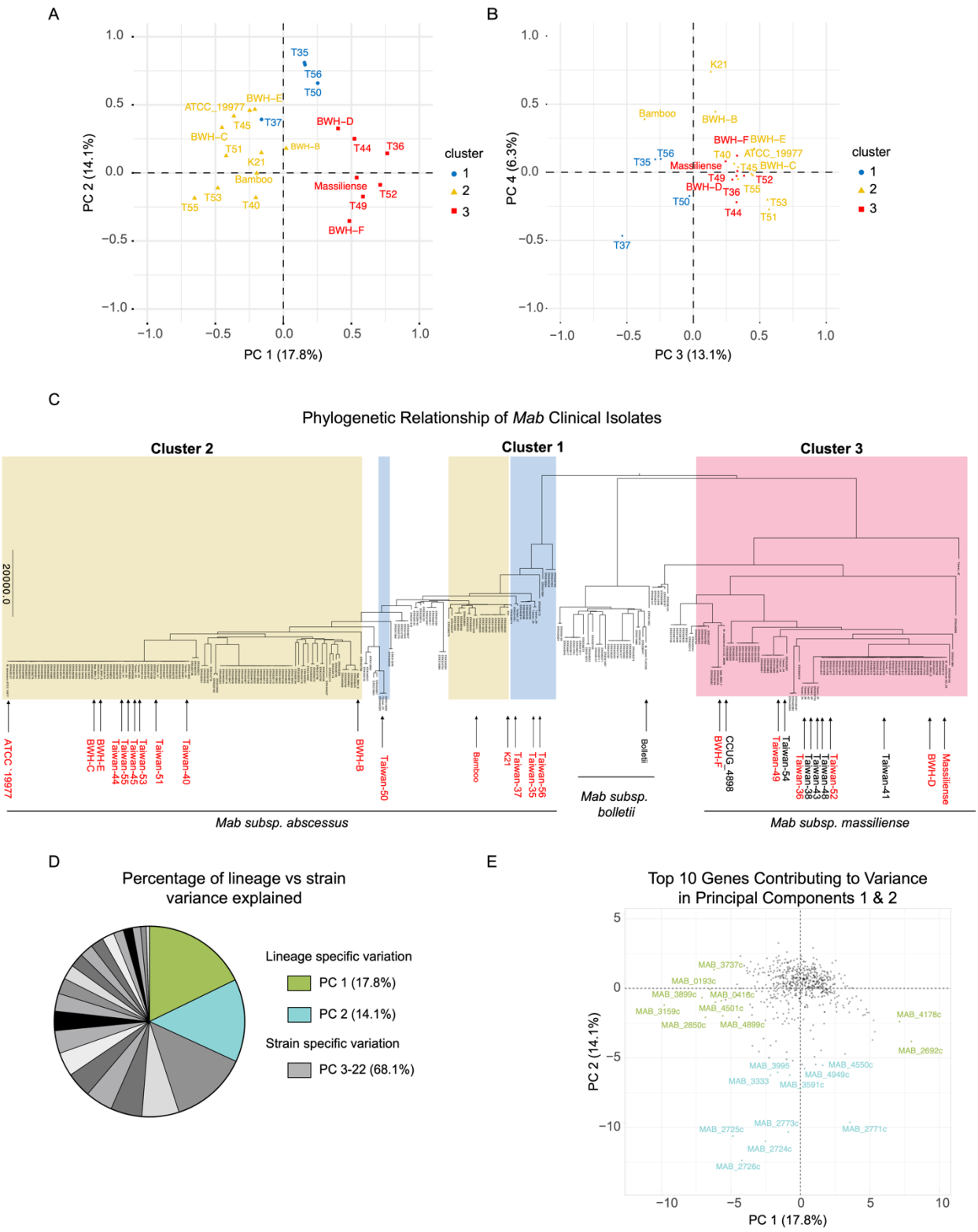

Figure 4: PCA of ANOVA Hits. (A) PC 1 & 2 of differentially required genes. **(B)** PC 3 & 4 **(C)** Phylogenetic tree of *Mab* clinical isolates shaded with rectangles highlighting clusters. **(D)** Percentage of variance explained by each of the principal components. **(E)** Plot depicting the top 10 contributing genes to the variance of PC 1 & 2

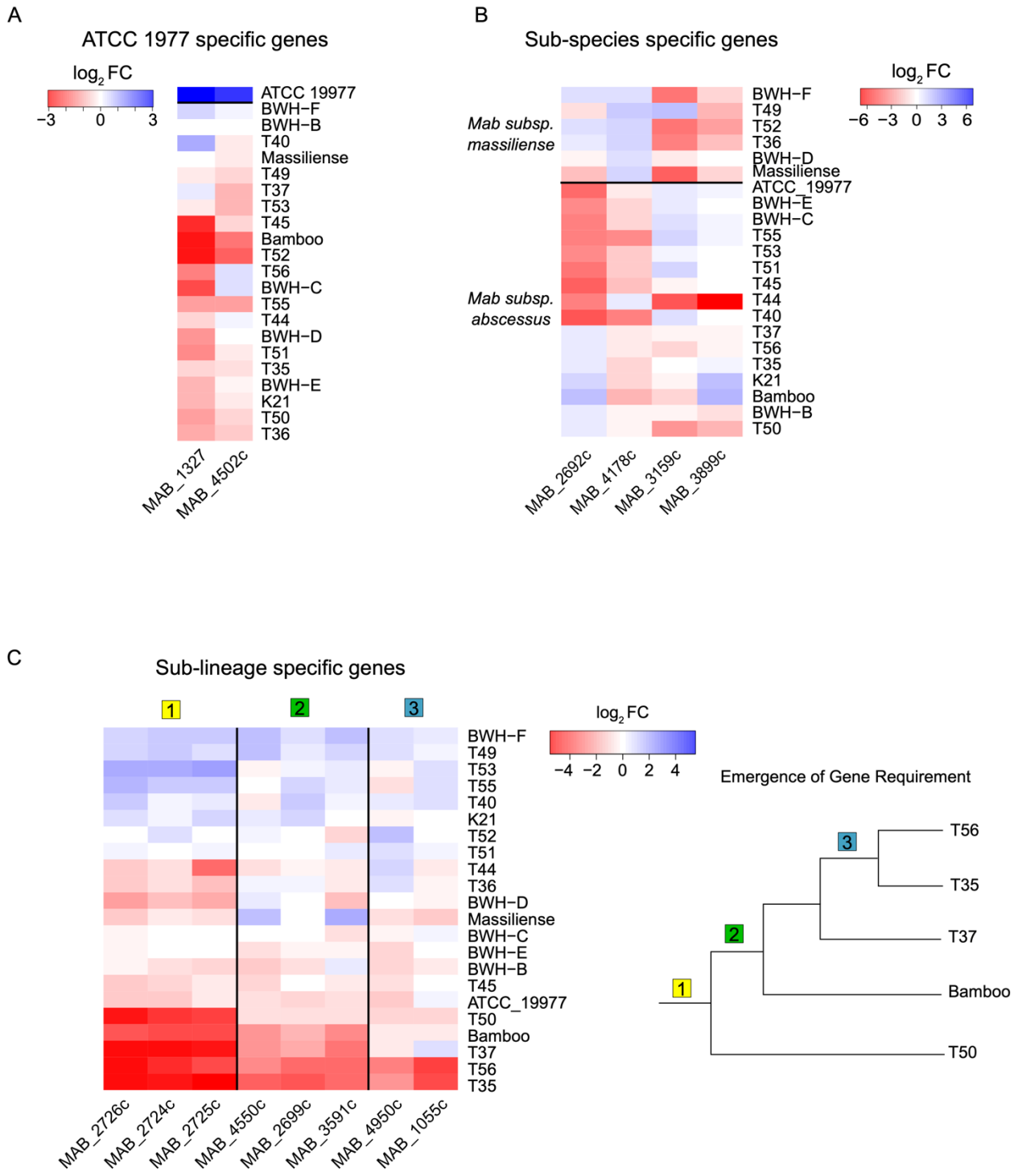

Figure 5: Sub-species and lineage specific genetic requirements (A) Genes specific to the reference ATCC 19977 strain **(B)** Genes that separate *abscessus* and *massiliense* sub-species. **(C)** (*left*) Differentially required genes in cluster 1. (*right*) Schematized phylogenetic relationship of cluster 1 strains

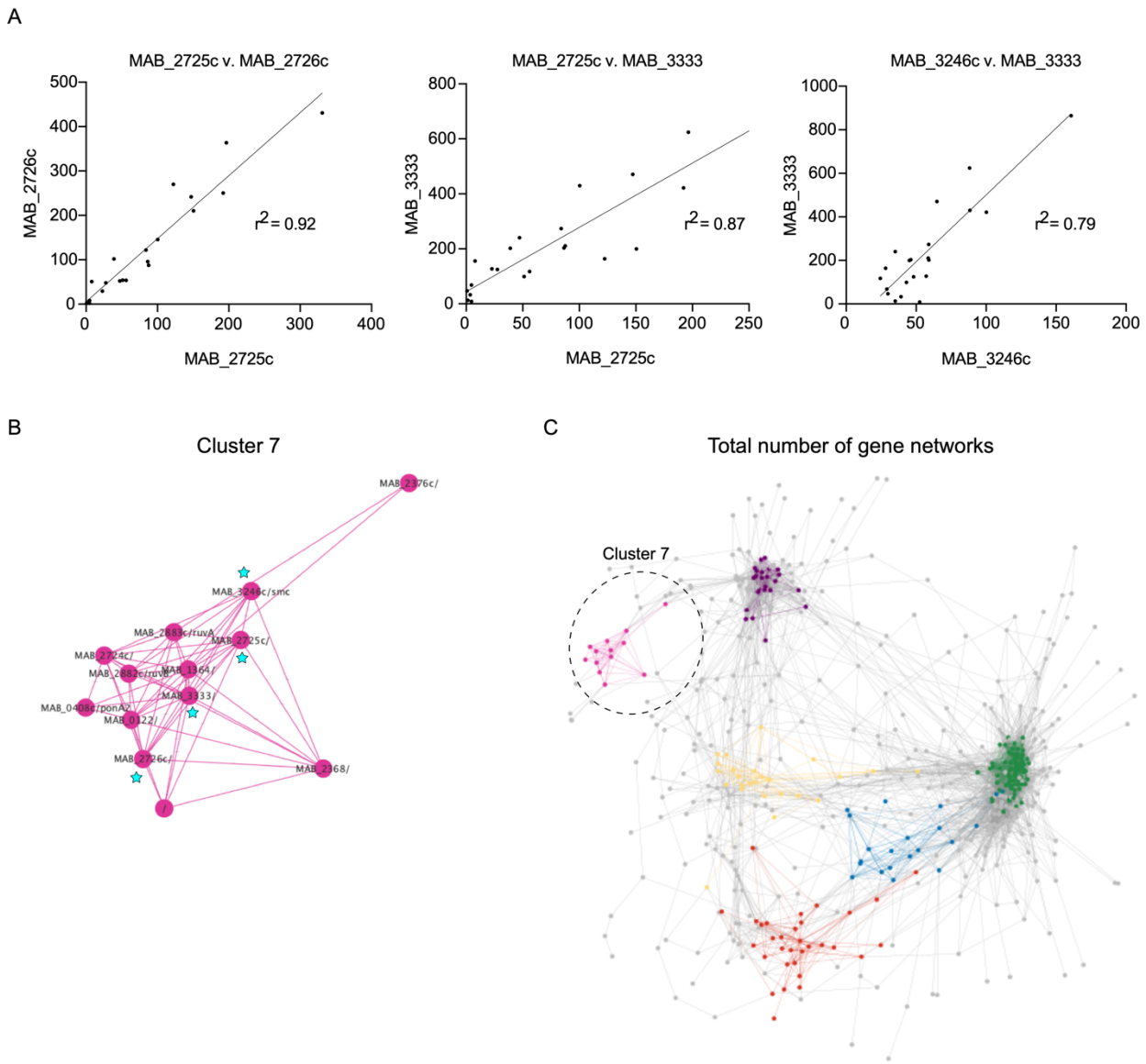

Figure 6: Network analysis of differentially required genes. (A) Correlation of transposon insertions between 3 gene pairs **(B)** Cluster 7 depicting 13 genes that are inter-correlated. Genes marked with blue stars are depicted in panel A. **(C)** Network analysis highlighting six additional clusters of a total of 19 identified. Cluster 7 is demarcated with a dashed circle

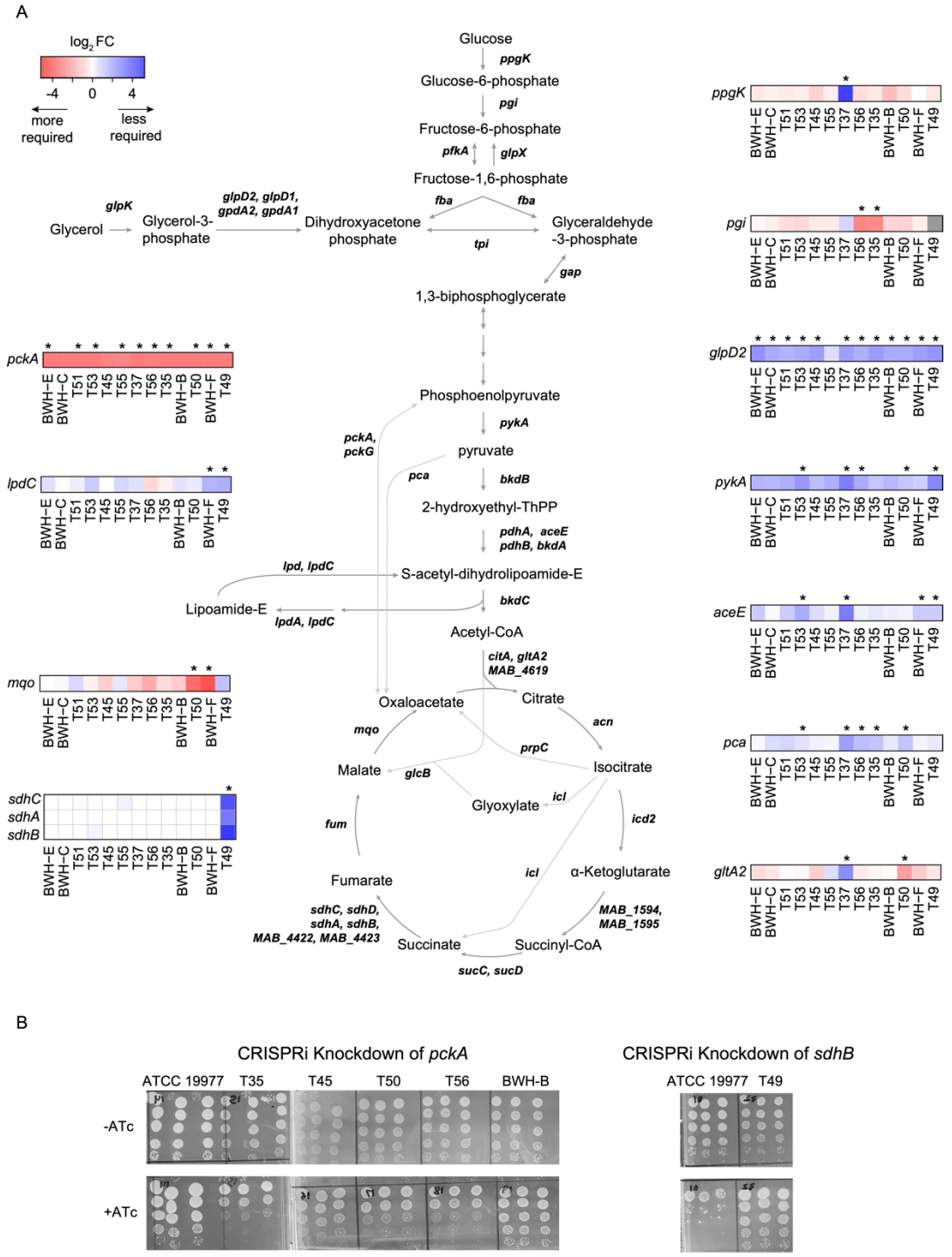

Figure 7: **TnSeq reveals differences in genetic requirement in carbon metabolism genes (A)** Schematic of genes in central carbon metabolism in *Mab*. Heatmaps showcase LFCs relative to the reference strain. Genes with significant differences in LFC are demarcated with a '*' indicating a p-adj < 0.05. **(B)** CFU plate data showing knockdown of *pckA* and *sdhB* using CRISPRi. +ATc induces gene repression

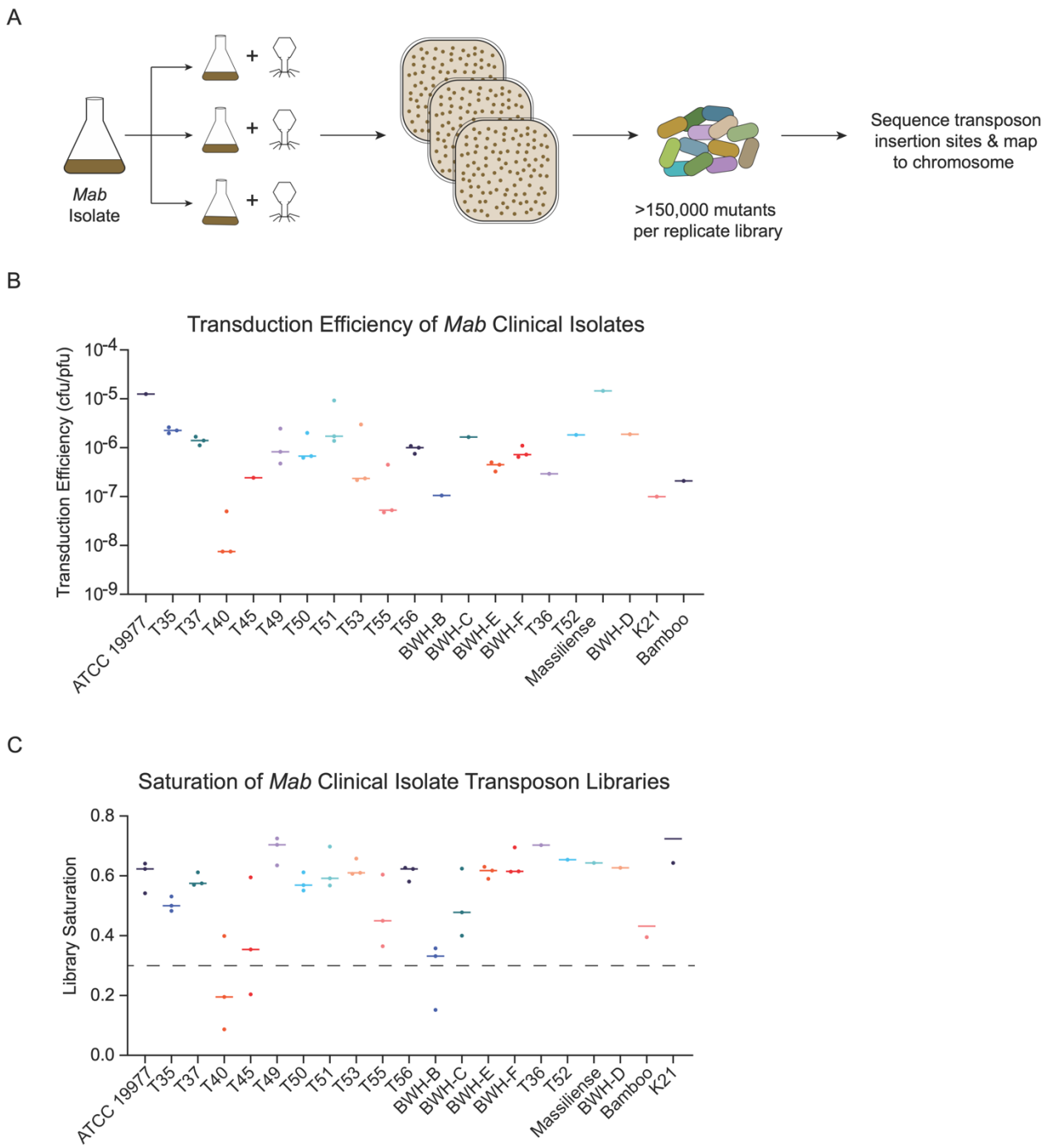

Supplemental Figure 1: Summary of TnSeq data. (A) Schematic of TnSeq experiment. **(B)** Transduction efficiency (cfu/pfu) of *Mab* clinical isolates. (**C)** Percent saturation of TnSeq libraries. Dotted line demarcates this 30% library saturation used as a threshold for inclusion in the study.

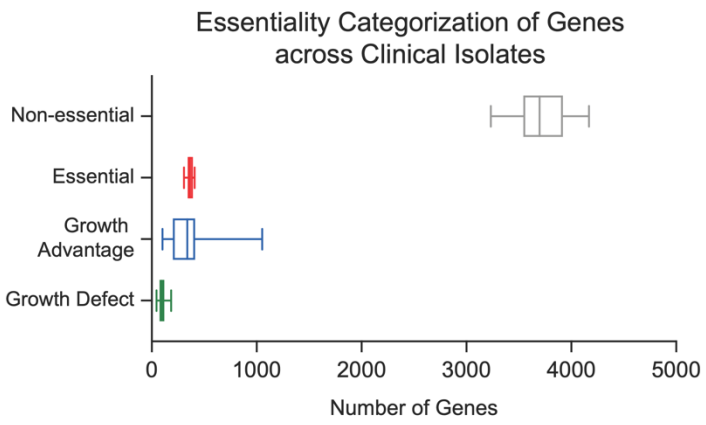

Supplemental Figure 2: Summary of gene essentiality data across 22 clinical isolates